Journal of Electroanalytical Chemistry 837 (2019) 151–158

Contents lists available at ScienceDirect

Journal of Electroanalytical Chemistry

journal homepage: www.elsevier.com/locate/jelechem

Laminated Lithium Ion Batteries with improved fast charging capability

Martin Frankenberger[a,*], Madhav Singh[a], Alexander Dinter[a], Sebastian Jankowksy[a], Alexander Schmidt[b], Karl-Heinz Pettinger[a]

[a] University of Applied Sciences Landshut, Technology Center for Energy, Wiesenweg 1, 94099 Ruhstorf, Germany
[b] Karlsruhe Institute of Technology (KIT), Institute for Applied Materials-Energy Storage Systems (IAM-ESS), 76344 Eggenstein-Leopoldshafen, Germany

ARTICLE INFO

Keywords:
Lithium-ion battery
Lamination
Fast charging capability
Fast discharge capability
Cell compression
Enhanced cycling stability

ABSTRACT

The fast charge and discharge capability of lithium-ion batteries is improved by applying a lamination step during cell assembly. Electrode sheets and separator are laminated into one stack which improves the electrochemical performance as well as the stack assembly process. The effect of non-laminated and laminated interfaces on the reversible capacity during cycling are studied thoroughly in half-cell and full-cell configurations. The fully-laminated cells show a reduction in the capacity losses of 3%, 5% and 12% upon cycling at 2C, 3C and 5C-rate, respectively, while capacity losses of 6%, 11% and 23% are observed in non-laminated cells at the same C-rates. A significant reduction in the capacity fading at high C-rates is observed upon lamination. Additional compression is applied on the cells to compare the effect of lamination and compression on the cell performance. The laminated cells show an improvement in the fast charging capability in comparison to the non-laminated cells.

1. Introduction

More than 40 years after production of the first commercial lithium cell by Sanyo in 1970s, [1] the lithium-ion battery (LIB) technology has become a main contributor for the storage devices in the field of rechargeable batteries. LIB technology needs further improvement in terms of fast charging capability which can reduce the charging time from hours to minutes especially for the electric vehicle applications. Enormous research is going on to improve the cell components such as active materials, [2,3] electrolyte, [4] separator [5,6] and manufacturing steps [7] in order to increase the energy density, power density, lifetime and reduce the cost. The performance of lithium-ion battery electrodes has been improved by varying the thickness [8,9] and porosity of the electrodes [10], controlling the stack pressure [11–15] and tuning the lithium ion diffusion paths in electrodes via modified manufacturing processes, for example by controlling the graphite particle orientation normal to the current collector surface during the coating step using a magnetic field, [16] or via laser structuring of graphite anodes, silicon/graphite anodes, NMC cathodes or $LiMn_2O_4$ cathodes [17–20].

The laser structuring creates additional lithium ion diffusion pathways and increases the active surface area of thick NMC and graphite electrodes, thus enhances the discharge capacities at higher C-rates [17,19]. Besides, LIB cycling stability and aging mechanism can also be improved by varying the stack pressure, [11–15] which influences the distribution of solid electrolyte interface (SEI) or plated lithium deposition on the graphite-separator interface [12,13,21]. It has been reported that the high stack pressure causes the higher capacity fade, so lower stack pressure is required to extend the life time. In addition, the non-uniform surface of the electrodes also induces non-uniform pressure at the interfaces among different electrode layers and the amplitude of the pressure varies during charging and discharging [11].

Non-uniform space among the electrodes and separator results in longer diffusion paths at the interfaces in the cell stacks, as shown in schematic Fig. 1a. In this regard, lamination technique stabilizes the electrode-separator interfaces, which shortens the lithium diffusion paths at the interfaces as well as stabilizing the active surface area of the electrodes during cycling significantly (Fig. 1b), and thus homogenize the liquid phase concentration [17] of the lithium ions on the active material particle surface. The lamination technique provides the slight mobilization of the polymer binder chains both in the separator and electrode by applying heat and pressure which interlinks the electrode-separator interfaces and also maintains the surface porosity of the electrode and the separator. The necessity for mobilization of polymer binder chains in all components limits the choice of binder to thermoplastic polymers with similar melting points. Heat-induced polymer chain mobilization must not exceed the melting temperature of the polymer in order to prevent the production of a nonporous interface

* Corresponding author.
E-mail address: martin-frankenberger@mytum.de (M. Frankenberger).

https://doi.org/10.1016/j.jelechem.2019.02.030
Received 19 September 2018; Received in revised form 29 January 2019; Accepted 15 February 2019
Available online 17 February 2019

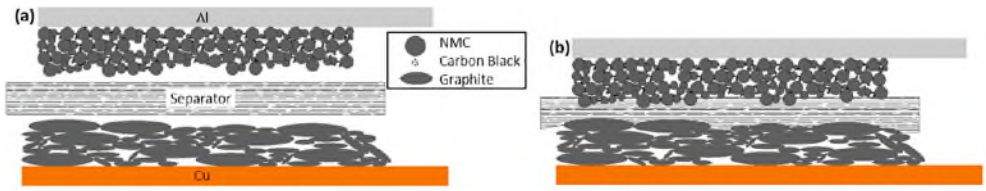

Fig. 1. Schematics of electrode-separator lamination technique; (a) non-laminated single cell stack (b) laminated single cell stack.

block.

Lamination technique has been well known for some decades [22,23] for the stacking process simplification which reduces the defects occurring due to electrode misplacement at the anode-separator-cathode compound [24]. Lamination technology connects the interlayers, separator-cathode and separator-anode, physically by using a roller lamination machine and therefore, maximizes the physical and ionic contacts as well as minimizing the voids at the interfaces (Fig. 1).

First time, the lamination technology was used in the assembly process during the lithium ion battery production in 1996 [22]. Later specific roller lamination technique was reported as a binding technique to prevent the air bubbles and wrinkles within the laminated material for preparing the supercapacitor electrode on a current collector [25]. Winding and lamination technologies are typically used as state-of-the-art technologies in industrial LIB production lines.

The lamination technique is a simple and easy-to-apply technology, which simplifies the stacking process by reducing the number of components. The lamination process enables fast assembly speeds up to 100 m/min and therefore lowers the costs of the assembly process. Besides, the lamination technique improves the electrochemical performance of the cell, in terms of improving cycling stability, reducing aging effects and stabilizing cell performance even in case of vacuum reduction in the cell, in comparison to the above mentioned additional electrode modification technologies.

In this article, we present a detailed study of the electrode-separator lamination in full cell configuration at higher C-rates. This study will reveal the significant improvement in the fast charging and discharging capability of single cells after applying the lamination technique.

2. Experimental

2.1. Materials

Commercially available battery grade cathode material $LiNi_{1/3}Mn_{1/3}Co_{1/3}O_2$ (NM-3102 h, *BASF,* Germany – former *TODA AMERICA,* USA) and anode material graphite (MAGE3, *HITACHI CHEMICAL*, Japan) were used as active materials. Conductive carbon (Super C65, *IMERYS,* Switzerland – former *TIMCAL*, Switzerland), cathode conductive graphite (KS6L, *IMERYS*) and anode conductive graphite (SFG6L, *IMERYS*) were used as conductive additives. PVDF (Solef® 5130, *SOLVAY*, Italy) was used as binder. *N*-methyl-pyrrolidone (*Overlack*, Germany) was used as solvent. 1 M $LiPF_6$ - ethylene carbonate (EC): ethylmethylcarbonate (EMC) 3:7 *w*/w (Selectilyte LP57, *BASF*, Germany) and vinylene carbonate (Vinylene Carbonate E, *BASF*, Germany) were used as electrolyte. A laminate type aluminum pouch film (*SHOWA DENKO AMERICA*, USA) was used as housing of pouch cells. Pure lithium and glass microfibre filter (Glass Fibre Filter Grade 691, *VWR-avantor*, USA) were used for T-cells (half-cell). A self-standing inorganic filled (Al_2O_3) separator film with a PVDF/HFP Copolymer as binding agent, was used for the pouch cell (full-cell) configuration. All materials and substrates were used as received.

2.2. Electrode/separator preparation

The cathode was prepared by mixing NMC (93 wt%), PVDF (3 wt%), Super C65 carbon (3 wt%) and KS6L graphite (1 wt%) with NMP by mixing MAGE3 graphite (90 wt%), PVDF (7 wt%), Super C65 carbon (2 wt%) and SFG6L graphite (1 wt%) with NMP to give a final solid content of 50 wt%. The electrode slurries were prepared in a planetary mixer (TX-2, INOUE, Japan) and were single-side coated by a doctor-blade coater in a roll-to-roll process coating machine. Electrodes were dried in-line in a two-step drying tunnel at the temperature range of 135–150 °C. Low electrode mass loadings were chosen to act as high capacity and high power reference system [26]. The averaged active mass loadings of cathode and anode electrodes were ~6.9 mg·cm^{-2} (1.13 mAh·cm^{-2}) and ~3.4 mg·cm^{-2} (1.28 mAh·cm^{-2}), respectively. The cathode and anode capacity balancing factor was 1:1.14 in the full cells. The electrodes in full cell configuration have mass in the range of 0.245–0.278 g of NMC and capacity in the range of 0.041–0.047 Ah.

2.3. Cell preparation

The active areas of cathode and anode sheets were 5 × 8 cm^2 and 5.4 × 8.4 cm^2 within the pouch cell. Cathode, anode and separator were laminated to make a single stack by using a lamination machine (BLE 282 D, *MANZ Italy* – former *ARCOTRONICS Italia S.p.A.*, Italy) at the roll speed of 1.38 m·min^{-1}, using a line force of 157 N·cm^{-1} in the temperature range 100–120 °C.

To analyze the effect of lamination on the electrochemical performance of cathode and anode individually, cathode-separator stacks were laminated by laminating a copper-separator-cathode stack, later the copper was replaced with the appropriate anode without any further lamination. Similarly, anode-separator stacks were laminated by laminating an aluminum-separator-anode stack, later the aluminum foil was removed from the stack, and replaced with the appropriate cathode without any further lamination. Nickel and aluminum tabs were welded onto the anode and cathode electrodes by ultrasonic welding. Pre-assembled pouch cell stacks were dried at 110 °C for 12 h under vacuum. The electrolyte amount of 500 µl for laminated cells and 750 µl for partially laminated/non-laminated cells is used within an argon filled glovebox (MB20, H_2O and O_2 content < 0.1 ppm, *MBraun*, Germany) and sealed under vacuum. The cells were kept at room temperature over night before starting the electrochemical characterization. To study the effect of additional cell compression, gravimetric force was applied to the cells by compressing each pouch cell stack with a weight of ~2.5 kg on top, while placing a polystyrol plate between the cell and applied weight for homogeneous force distribution along the active single cell area.

For half-cell measurements, the electrodes were punched into circular disks of 10 mm diameter and dried at 110 °C under vacuum for 12 h. Half-cell measurements were carried out in three electrode geometry using a Swagelok type T-cell setup, assembled in an Argon filled glovebox. Lithium metal was used as reference and counter electrode. LP57 was used as electrolyte for NMC half-cell measurements. A mixture of LP57 (98 wt%) and vinylene carbonate (2 wt%) was used as electrolyte for graphite half-cell measurements and for all full cell measurements. Half-cells were kept at room temperature over night before starting the electrochemical characterization.

2.4. Cell characterization

Electrochemical characterization was done with a battery tester

potentiostatic (CV) modes for charging step and CC-mode for discharge step. For full cell measurements, the voltage ranges were adjusted to 3.0 V–4.2 V, for NMC half-cell measurements the voltage ranges were adjusted to 3.0 V–4.3 V, for graphite half-cell measurements the voltage ranges were adjusted to 0.02 V–1.5 V. CV charging steps were continued until the charging current dropped below 0.05C rate. For the full cell experiments, formation was done by applying two cycles at 0.1C, calculated from the NMC weight and the theoretical NMC capacity of 168 $mAh{\cdot}g^{-1}$. For the further cycling process, C-rates were calculated according to the measured nominal capacity of each cell, which is the discharge capacity of the second formation cycle (see supplementary information). For half-cell experiments, the C-rate currents were calculated to fit to the theoretical capacity of the active material weight within the samples, using a theoretical NMC capacity of 168 $mAh{\cdot}g^{-1}$ and a theoretical graphite capacity of 372 $mAh{\cdot}g^{-1}$.

Non-laminated single cell components were prepared for cross-section images with a handheld punch (clearance 4 µm, *NOGAMI*, Japan). Argon ion cutting (EM TIC 3X, Leica, Germany) was used for the laminated electrode-separator stack. A field emission scanning electron microscope (FE-SEM) (Merlin Compact, *Zeiss*, Germany) with energy dispersive X-ray spectroscopy (EDX) was used to take cross-section images and EDX element mapping images of a laminated single cell stack.

Porosities of separator and electrode layers were calculated by comparing their real volume with the minimal component volume given by the sample weight, using the theoretical densities of the components.

$$\text{Porosity} \quad \frac{\text{pores}}{\text{real}} \quad \frac{\text{real} - \text{components,minimal}}{\text{real}} \tag{1}$$

For impedance spectroscopy analysis, full cells were charged to 3.6 V at 0.1C rate directly after formation. Impedance measurements were carried out in a climate chamber (INCU-Line® IL 68R, *VWR-avantor*, USA) at 25 °C. After connecting to the potentiostat (PGSTAT204, *Metrohm Autolab*, Netherlands), the cells rested for 2 h at 25 °C prior to the measurement. Impedance analysis was done in potentiostatic mode in the frequency range of 50 kHz–10 mHz using an amplitude of 10 mV. Data fitting was performed using *Z*-fit.

3. Results and discussion

3.1. Morphological characterization

Fig. 2 shows the cross-section SEM images of the non-laminated single cell components NMC cathode, self-standing inorganic filled separator film and graphite anode.

Cross-section SEM and EDX images of a laminated single cell stack, containing NMC cathode, self-standing inorganic filled (Al_2O_3) separator film and graphite anode, are shown in Fig. 3.

The cross-section images of interfacial linking with both electrodes clearly show the correspondence with the schematics, as shown in Fig. 1. No remaining voids are visible at the interfaces (cathode/separator and anode/separator interfaces) while the separator surface clings to NMC surface particles at the cathode side and to graphite surface particles at the anode side. The high magnification image, Fig. 3b and Fig. 3c, show that NMC/graphite particles and separator adhere perfectly after lamination. It could be mentioned that no damaging of active materials were found during the lamination process. In addition, lamination provides stabilized interfaces which minimize the interfacial resistances and reduce the capacity fading upon increasing the C-rates. The EDX image proves that the electrode and separator interface is well contacted. The EDX mapping shows the homogeneous distribution of alumina in the separator (Fig. 3d).

The overall pore volume within the active area of anode layer, separator and cathode layer in the single cell stack is reduced by ~66% separator-anode stack decreases from ~54% down to ~30%. The SEM images show the pore volume loss to primarily occur via particle reorganization at the electrode-separator interface.

3.2. Half-cell measurements

NMC cathode and graphite anode are electrochemically tested in half-cell configuration versus lithium metal. Both electrodes reflect the nominal capacities as specified by the manufacturers, and show negligible capacity losses upon cycling at different C-rates (see Fig. S2 in Supplementary information). These optimized electrodes are used to study the effect of lamination and compression on the electrochemical performance in full cell configuration.

3.3. Full cell measurements

3.3.1. Electrochemical performance of laminated cells

To identify the influence of the electrode-separator lamination on the electrochemical performance, non-laminated cells are compared with fully laminated cells. Specific influence of the individual interface lamination of anode-separator and cathode-separator are studied by comparison of partially laminated stacks. The counter electrodes in non-laminated and partially laminated full cells are hold in position by the pouch foil housing in the evacuated cell.

To study the significant influence of the lamination on the charging and discharging capacities of the full-cells, the cells are charged at fixed C-rate while discharged at variable C-rates and vice-versa, as shown in Fig. 4. The charge-discharge curves of laminated and non-laminated cells at charge and discharge rate tests are given in supplementary information. From the relative discharge capacity graphs, Fig. 4a, it can be seen that the lamination process on both interfaces has significantly improved the capacities especially at higher C-rates. In addition, the overall electrochemical performance also improves at mild C-rates after lamination. The cells show that the difference in the discharge capacity values is not changing up to 0.5C rate, while at higher C-rates the discharge capacity ratio is significantly high. The non-laminated cell reveals 72% of the nominal capacity, while the laminated cell shows 84% of the nominal capacity at 5C rate. Besides, the cells show hardly any influence of the C-rate on the charge/discharge capacities and recover the initial capacities even after cycling at 5C-rate. In addition, partially laminated cells such as anode-separator lamination and cathode-separator lamination also show slight improvement in the discharge capacity at high C-rates. It indicates that the advantages of the lamination can be only seen when the cell is fully laminated at both interfaces. The laminated cell at 5C-rate delivers even slightly higher discharge capacity in comparison to the non-laminated cell at 3C-rate.

Charge capacity graphs, Fig. 4b, indicate that charge rate tests show no significant difference in the cell performance, revealing 94–96% of the nominal capacity, at various C-rates especially upon applying CCCV-mode, which results from the same cut-off current 0.05C. Therefore any overpotential differences between the cells are neglected (see Fig. S7 in SI). On the other hand, the capacity fractions during charging in CC-mode show similar improvement in CC charge rate stability upon lamination, as observed in the discharge rate tests, Fig. 4a. The non-laminated cell charges 55% of the nominal capacity in CC-mode, while the capacity increases to 70% upon lamination at 5C charge rate. This indicates a clear improvement in the fast-charging capability of the cell upon electrode-separator lamination. As can be seen from Fig. 4, the CC-charge mode delivers slightly lower capacities in comparison to CC-discharge mode which could be due to the unequal kinetics of graphite lithiation and delithiation at different C-rates. Partially laminated cells reveal 55% of the nominal capacity upon anode laminated and cathode laminated stacks charged at 5C-rate in CC-mode. The results again prove that no improvement in the electrochemical performance of the cell is observed upon partial lamination

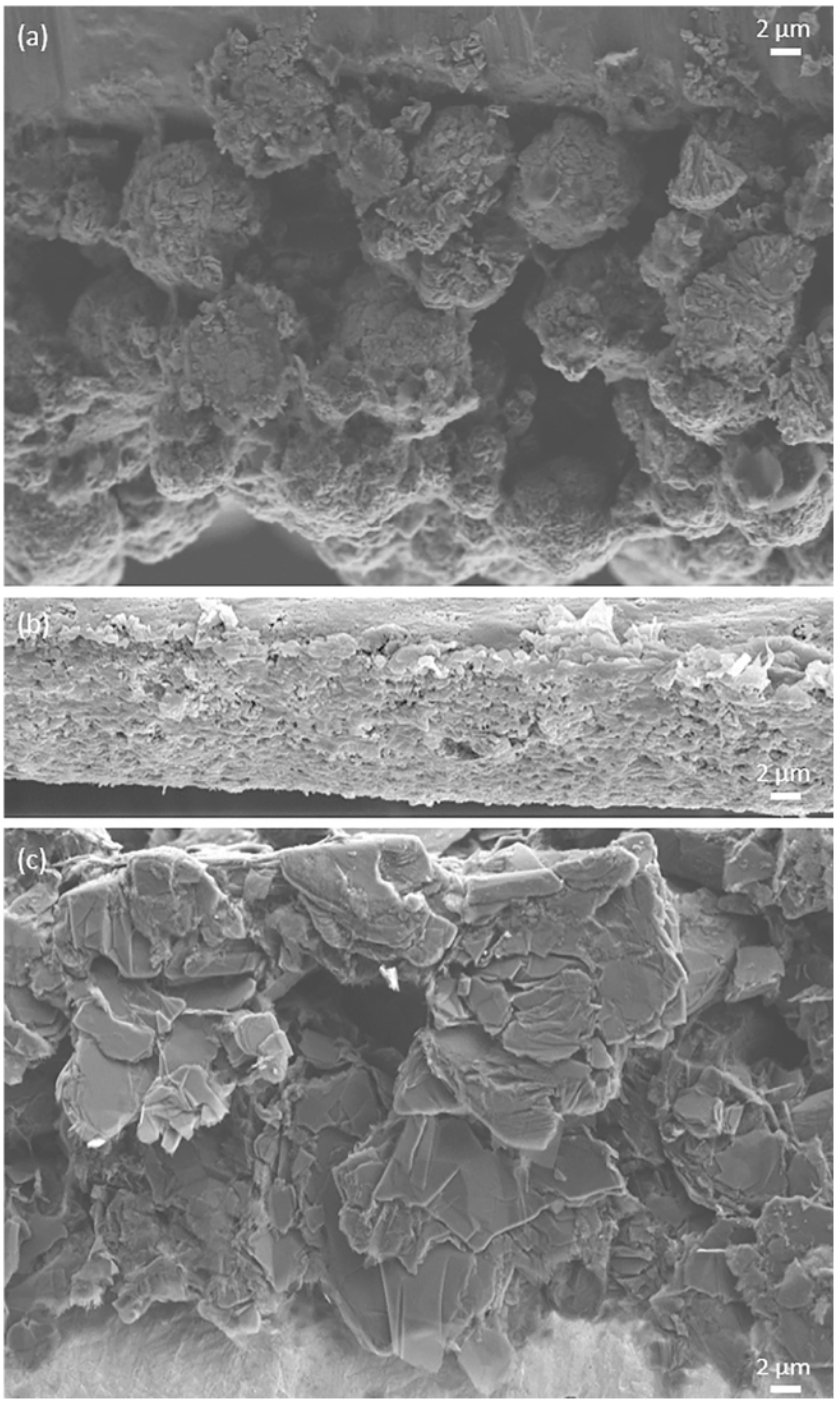

Fig. 2. Cross-section SEM images of non-laminated stack components (a) NMC cathode; (b) self-standing inorganic filled separator film; (c) graphite anode.

From the results of charge and discharge rate tests, it proves that the electrode-separator lamination technique improves the fast charging and discharging capability of the cell. Lamination process improves the pore structure at both interfaces, as shown in the SEM images in Fig. 3, which provides a better ionic network as well as physical contacts among the particles and separator at the interfaces. It would be worth mentioning here that the lamination shortens the ionic path length especially at the electrode-separator interfaces, thus improving the charge and discharge rate capability, see Fig. 4.

3.3.2. Influence of additional stack compression

In multilayer electrode stacks additional compression besides the compression from the adjacent cells. In this regard, to investigate the effects of electrode-separator lamination in multilayer stack, additional analysis is necessary. To compare the effects of compression and lamination on the electrochemical performance in single cells, an additional gravimetric force is applied on the pouch cells. The internal cell pressure of the as-built cell with electrolyte is 43 mbar at 25 °C. Additional gravimetric cell pressure is realized at 143% of the internal cell pressure. Charge and discharge rate tests are performed with a corresponding single cell series of non-laminated cells and fully laminated cells after applying additional compression.

A comparison study is done to analyze the effect of additional compression along with lamination and non-lamination process, as

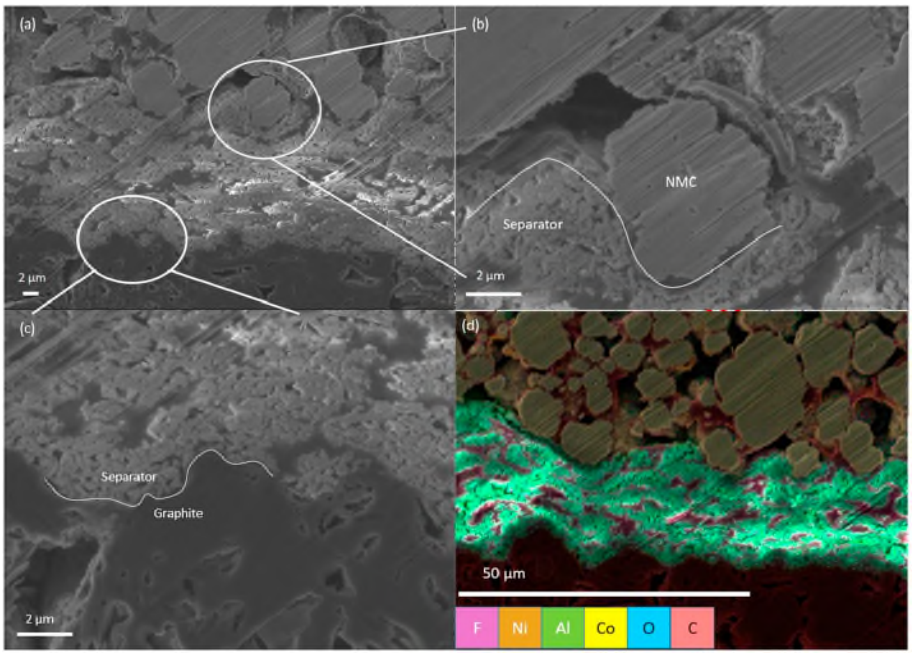

Fig. 3. Cross-section images of laminated single cell stack: NMC cathode in upper part, self-standing inorganic filled separator film in central part, graphite anode in lower part; (a, b, c) SEM image, recorded at a voltage of 5.0 kV and a working distance of 13 mm (d) EDX element mapping image.

laminated cells at charge and discharge rate tests in additional compressed and uncompressed states are given in supplementary information. As it has been mentioned earlier, the non-compressed cells show differences in the C-rate stability. The non-laminated cell shows slight improvement in the C-rate stability after applying additional pressure to the cells, resulting in 80% of the nominal capacity at 5C discharge mode. In addition, the cells show hardly any influence of the C-rate on the charge/discharge capacities and recover the initial capacities even after cycling at 5C-rate.

Discharge capacity values clearly indicate that the additional compression does not have an obvious effect on the laminated cells, while non-laminated cell shows significant improvement in the discharge capacity in comparison to the uncompressed non-laminated cell.

The charge capacities in CCCV-mode lie in the range of 94–96% of the nominal capacity along all cell geometries and C-rates (see Fig. S7 in SI), while the CC-charge capacities show the same trend like the discharge capacities. Additional compression on the non-laminated cell improves the charge rate stability in CC-mode and raises the capacity from 54% to 66% at 5C-rate, while the laminated cell provides 70% of the nominal capacity in both non-compressed and compressed states at the same C-rate. From the results of discharge rate and charge rate capability tests, it is clear that the cell compression and lamination processes improve the cell performance. From the results it is clear that the additional compression also slightly improves the physical contacts among the electrode-separator interfaces. Lamination technology has advantages at microscopic level in comparison to the additional gravimetric cell compression. Lamination technique improves the pore structure upon mobilization of the polymer chains in the electrode and separator, resulting the better ionic network in addition to the better physical contacts at both interfaces. It has been reported that the cycling efficiency of lithium-ion cells is strongly affected by applying additional stack pressure [11–15,27]. The stabilization in the cycling efficiency was shown to arise from modified SEI growth at compressed state [11–15,27].

3.3.3. *Fast charging and fast discharging cycling test*

Cycling studies are performed on non-laminated and fully laminated cells to evaluate the long-term effects of the indicated discharge and

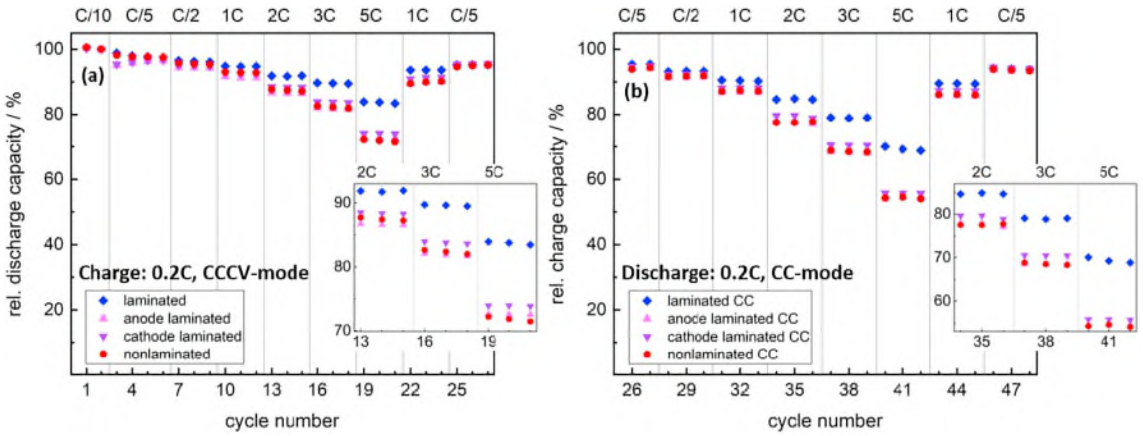

Fig. 4. C-rate tests of uncompressed single cells; (a) discharge capacities of discharge rate test, discharge rate per step as indicated, charge rate: 0.2C, CCCV-mode; (b)

DOCKET ALARM

Explore Litigation Insights

Docket Alarm provides insights to develop a more informed litigation strategy and the peace of mind of knowing you're on top of things.

Real-Time Litigation Alerts

Keep your litigation team up-to-date with **real-time alerts** and advanced team management tools built for the enterprise, all while greatly reducing PACER spend.

Our comprehensive service means we can handle Federal, State, and Administrative courts across the country.

Advanced Docket Research

With over 230 million records, Docket Alarm's cloud-native docket research platform finds what other services can't. Coverage includes Federal, State, plus PTAB, TTAB, ITC and NLRB decisions, all in one place.

Identify arguments that have been successful in the past with full text, pinpoint searching. Link to case law cited within any court document via Fastcase.

Analytics At Your Fingertips

Learn what happened the last time a particular judge, opposing counsel or company faced cases similar to yours.

Advanced out-of-the-box PTAB and TTAB analytics are always at your fingertips.

API

Docket Alarm offers a powerful API (application programming interface) to developers that want to integrate case filings into their apps.

LAW FIRMS
Build custom dashboards for your attorneys and clients with live data direct from the court.

Automate many repetitive legal tasks like conflict checks, document management, and marketing.

FINANCIAL INSTITUTIONS
Litigation and bankruptcy checks for companies and debtors.

E-DISCOVERY AND LEGAL VENDORS
Sync your system to PACER to automate legal marketing.